Catalytic Janus Motors on Microfluidic Chip: Deterministic Motion for Targeted Cargo Delivery

Larysa Baraban,[†,*,#] Denys Makarov,[†] Robert Streubel,[†,‡] Ingolf Mönch,[†] Daniel Grimm,[†] Samuel Sanchez,[†,*] and Oliver G. Schmidt[†,‡]

[†]Institute for Integrative Nanosciences, IFW Dresden, Helmholtzstrasse 20, D-01069 Dresden, Germany, and [‡]Material Systems for Nanoelectronics, Chemnitz University of Technology, Reichenhainer Strasse 70, D-09107 Chemnitz, Germany. [#]Present address: Max Bergmann Center of Biomaterials, Dresden University of Technology, Budapester Strasse 27, D-01069 Dresden, Germany.

ABSTRACT

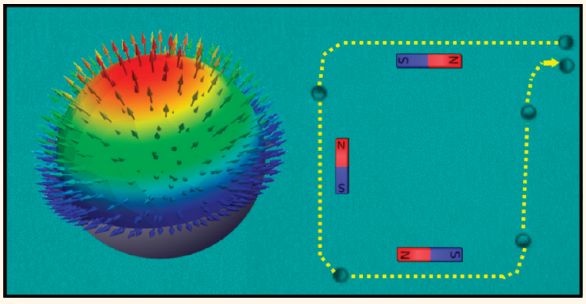

We fabricated self-powered colloidal Janus motors combining catalytic and magnetic cap structures, and demonstrated their performance for manipulation (uploading, transportation, delivery) and sorting of microobjects on microfluidic chips. The specific magnetic properties of the Janus motors are provided by ultrathin multilayer films that are designed to align the magnetic moment along the main symmetry axis of the cap. This unique property allows a deterministic motion of the Janus particles at a large scale when guided in an external magnetic field. The observed directional control of the motion combined with extensive functionality of the colloidal Janus motors conceptually opens a straightforward route for targeted delivery of species, which are relevant in the field of chemistry, biology, and medicine.

KEYWORDS: catalytic engines · synthetic micromotors · Janus particles · cargo delivery · perpendicular magnetic anisotropy · microfluidics

The development of smart artificial machines[1−7] is fast and, by now, they have been used in various biochemical assays for transportation and release of cells,[8,9] molecules,[10] or even for integration into the human body for targeted (drug) delivery.[11,12] Among the large family of man-made engines, self-propelled catalytic motors capable of transforming chemical energy into mechanical power at the micro- and nanoscale are one of the most dynamically developing classes of synthetic machines.[5,6,13−19] Currently available catalytic motors spanning from nanorods[13−15] and plates,[16] tubular jet-engines,[17,18,20] to metallic and dielectric particles[21,22] are asymmetrically decorated with a catalyst that triggers the decomposition of hydrogen peroxide into water and molecular oxygen and, in turn, induces the autonomous motion of the particles.

Colloidal microbeads are very attractive for the field of artificial machinery, as they have already found numerous *in vitro* and *in vivo* applications, for example, for immunoassays,[23,24] biodetection,[24,25] and targeted drug delivery,[12,26] and have a great potential to be used for efficient cancer treatment.[27] The advantages of this type of catalytic engines are intriguing: they are easy to fabricate; their production is cheap; and the properties of these objects can be tuned *via* functionalization.[26] Furthermore, such spherical particles can acquire catalytic properties that allows them to act as synthetic self-powered micromotors.[27,28] The motion of Janus particles is strongly influenced by Brownian diffusion.[21,28] Although the self-propulsion of such catalytic motors has already been reported, their *directed* motion, which is required for delivery applications, has not been achieved so far.

A deterministic motion of catalytic engines can be obtained by applying an external magnetic field.[28,29] Interestingly, the approach described in literature for guiding magnetic catalytic motors (nanorods and microtubes) consisting of materials with *in-plane* easy axis of magnetization (*e.g.*, Fe or Ni films) cannot be applied to spherical Janus particles due to their high symmetry. The fixed orientation of the magnetic moment of all known catalytic engines relies on the magnetic shape anisotropy of tubular[29] or rodlike objects.[30] To produce such objects, complex multistep fabrication

* Address correspondence to larysa.baraban@nano.tu-dresden.de, s.sanchez@ifw-dresden.de.

Received for review January 28, 2012 and accepted March 16, 2012.

Published online March 16, 2012
10.1021/nn300413p

procedures have to be applied involving lithography or porous membranes used as templates.

Here, we go beyond the well-known fabrication methods of spherical catalytic Janus particles providing them with special magnetic cap structures capable of acquiring directed motion. This new concept relies on the specific properties *of ultrathin magnetic multilayers* deposited onto the spheres, but not on the shape of the motor. The deterministic behavior of the motors in an applied magnetic field is guaranteed as long as the magnetic film possesses a well-defined *perpendicular* magnetic anisotropy (magnetic moment points perpendicular to the sample surface) in contrast to the usually applied layers with *in-plane* magnetic easy axis.[29,30] Magnetic materials with perpendicular anisotropy are known and widely applied to conventional magnetic data storage.[31−33] Among them, $[Co/Pt(Pd)]_N$ multilayer stacks are the most attractive for our purpose, since they exhibit the required magnetic properties when grown at room temperature on virtually any substrate.[34−37] In this respect, it was reported that $[Co/Pt(Pd)]_N$ stacks reveal perpendicular magnetic anisotropy even when deposited on arrays of spherical particles with sizes ranging from 50 nm to 5 μm.[38−42]

We demonstrate the autonomous propulsion of the magnetically modified catalytic Janus particles when soaked in hydrogen peroxide solutions as well as their precise steering in microfluidic channels for the manipulation (uploading, transportation, and delivery) of microobjects.[28,29,43,44] We further show that the motion can be stopped on demand *via* spatially changing the magnetic field orientation. Moreover, the Janus motors are sufficiently powerful to carry large loads and multiple particles.

RESULTS AND DISCUSSIONS

Fabrication of Catalytic Magnetic Janus Particles. The fabrication of catalytic Janus motors includes two steps: bottom-up self-assembly of microscopic particles and the deposition of the magnetic layer system. The resulting colloidal structures exhibit high symmetry, while the procedure is simple and cost efficient. Large arrays of spherical silica colloids (diameter of 5 μm, Bangs Laboratories) are conventionally prepared by dripping the suspension onto a clean glass substrate, followed by slow evaporation of the solvent under ambient conditions.[45] Afterward, the samples with the particle array are introduced to the vacuum chamber (base pressure of 1×10^{-7} mbar). The deposition of the magnetic multilayer stack consisting of [Co(0.4 nm)/Pt(0.6 nm)]$_5$ is carried out at room temperature (Ar sputter pressure, 8×10^{-3} mbar) by means of dc magnetron sputtering. To improve the growth conditions of the $[Co/Pt]_5$ multilayers, a 2-nm-thick Pt buffer layer is sputtered prior to the multilayer stack. Finally, a 15-nm-thick Pt layer is deposited to protect the multilayer stacks from oxidation and to preserve the catalytic nature of the particles toward the decomposition of H_2O_2. The scanning electron microscopy (SEM) micrograph in Figure 1a shows the monolayer of particles after the metal layer stack was deposited. The metal film forms caps on top of the silica particles (inset in Figure 1a). The fabrication of large arrays of catalytic Janus particles can be easily realized without using expensive patterning technologies.[46] Furthermore, the fabrication technique can be applied to both micro- and nanoscopic spherical particles, which substantially extends the size range of produced catalytic engines.

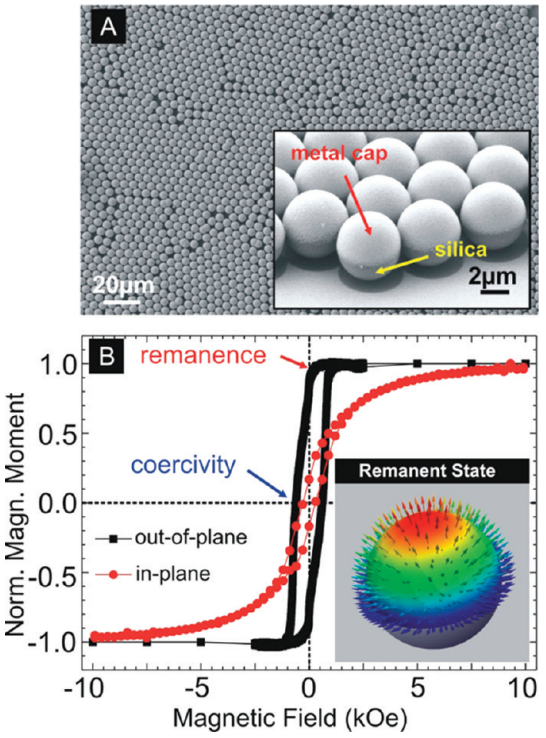

Figure 1. (a) Scanning electron microscopy image revealing an array of self-assembled spherical particles (diameter, 5 μm). The inset shows the coating of the Janus particles with metal film assuring their catalytic (topmost Pt layer) and magnetic properties ($[Co/Pt]_5$ multilayer stack). (b) Magnetic characterization using SQUID magnetometry of an array of spherical Janus particles covered by the $[Co/Pt]_5$ multilayer stack. Measurements are carried out in an in-plane and out-of-plane magnetic field. Coercive field and remanent magnetic moment are indicated with blue and red arrows, respectively. The inset shows schematically the distribution of magnetic moments in the cap at remanence after magnetic saturation. The resulting magnetic moment is oriented along the main symmetry axis of the cap structure.

The magnetic properties of Janus particles were investigated at room temperature with the aid of a superconducting quantum interference device (SQUID) in the range of ±70 kOe. The magnetization reversal processes were measured for both in-plane and out-of-plane magnetic fields revealing perpendicular magnetic anisotropy for $[Co/Pt]_5$ multilayers grown onto ensembles of spherical particles (Figure 1b). The coercive field of the magnetic sample (blue arrow in Figure 1b) is about 600 Oe. After being

exposed to an out-of-plane magnetic field, the sample preserves high remanent magnetization (red arrow in Figure 1b). This property is used to ensure a well-defined magnetization of each sphere by *magnetic saturation* of the sample before detaching from the substrate. The inset in Figure 1b schematizes the distribution of magnetic moment in a cap after saturation (remanent state). The orientation of the average magnetic moment of the cap coincides with its main symmetry axis. Consequently, the direction of the motion of catalytic Janus motors can be controlled at large scale by an external magnetic field. Changing the orientation of the magnetic field with a magnitude smaller than the coercive field, results in a rotation of the whole Janus particle but not in a reorientation of its magnetic moment.

After fabrication, capped particles are detached from the glass substrate by sonication and suspended in an aqueous solution of hydrogen peroxide. Further, 200 μL of this colloidal suspension with 10 wt % of H_2O_2 is dripped onto a previously cleaned glass substrate. Since the particles settle fast due to the gravity and perform the motion only at the glass substrate, we consider their motion as quasi 2-dimensional.[47] The moving particles were observed while exposed to an applied magnetic field using video-microscopy and recorded with a high-speed camera (Zeiss AxioCam HSm).

Characterization of the Motion of Individual Janus Particles. In the following, we present a quantitative analysis of the self-propulsion of such catalytic particles, caused by the decomposition of hydrogen peroxide on the metal caps, which is attributed to a self-diffusiophoretic mechanism.[48,49] We will further demonstrate the possibility to control the motion of such catalytic motors by applying a weak external in-plane (parallel to *x*- or *y*-axis) or out-of-plane (along *z*-axis) magnetic field. Figure 2 illustrates the studies of the dynamic properties of free, single catalytic particles in an external in-plane magnetic field (*xOy* plane). First, we investigate the dependence of the velocity V_{mean} of the catalytic Janus spheres on the concentration of the fuel molecules in the solution (Figure 2a). The mean value V_{mean} is determined from instantaneous velocities $\langle V(t) \rangle$ of six catalytic particles (details on evaluation and statistical analysis, including velocity distribution are in the Supporting Information). The velocity of the particles increases and tends to saturate for higher concentrations of H_2O_2, representing the gradual saturation of the catalytic centers at the surface of a cap.

The application of a small external magnetic field below 10 Oe is sufficient to align magnetic moments of the caps with respect to the magnetic field *via* physical rotation of the spheres. Note that the strength of the field used for particle manipulation is substantially smaller than the measured coercive field (about 600 Oe), which is required to switch the orientation of the

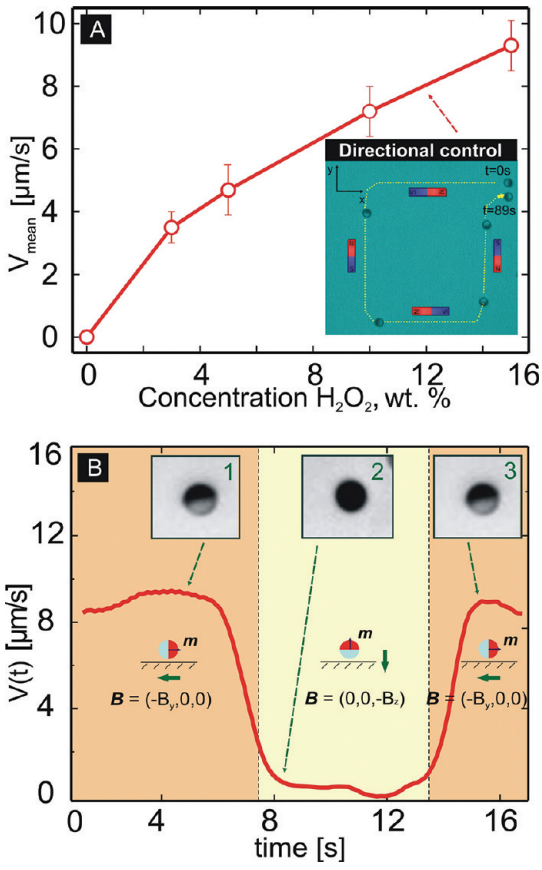

Figure 2. Catalytic properties and control of the motion of the Janus engines. (a) Dependence of the mean velocity of the Janus motor upon the concentration of H_2O_2 fuel in the solution. Additional statistical analysis is provided in the Supporting Information. The inset shows the deterministic motion of the catalytic magnetic Janus motor when guided using an external magnetic field. Trajectory of the capped particle as well as orientation of the magnetic field is indicated. (b) Controlled motion of the Janus particles can be achieved by orienting external magnetic field either in-plane (deterministic propulsion with a certain velocity, regions 1 and 3) or out-of-plane (particle stops, region 2).

magnetic moment of a cap. The reorientation of the particles in the applied field is visualized by tracing the contrast between nontransparent metal cap and transparent silica side (insets in Figure 2a,b). The magnetic field is applied in an alternating manner along the *x*- or *y*-axis, which leads to a corresponding reorientation of the direction of motion as revealed by square-like trajectories in the inset of Figure 2a and shown in Supporting Information, Movie 1. The applied magnetic field eliminates the rotational diffusion of Janus particles, and their motion becomes directionally deterministic. Interestingly, the magnetically controlled Janus motors can not only change the direction, but also stop their motion on demand, as shown in Figure 2b, when the orientation of the external magnetic field is alternated between *y* or *z*-axis (Supporting Information, Movie 2). For demonstration, catalytic Janus particles were suspended in 10 wt % aqueous

solution of hydrogen peroxide. The in-plane (*y*-axis) magnetic field orients the magnetic cap of the sphere parallel to the substrate (snap 1 in Figure 2b) allowing its catalytic motion with a velocity of about 8 μm/s. On the contrary, applying the magnetic field along the *z*-axis (*i.e.*, perpendicular to the glass plane) aligns the magnetic cap perpendicularly to the substrate (snap 2 in Figure 2b) that causes a complete stop of the particle. Further application of the in-plane field leads to the reorientation of the particle (snap 3 in Figure 2b) and recovery of its initial motion.

Targeted Cargo Delivery. Here, we show the ability of the catalytic Janus motors to perform advanced tasks, that is, targeted cargo delivery (Figure 3). In this experiment, a solution containing cargo beads [chemically inert superparamagnetic spherical particles (Sigma Aldrich)] of 10 μm diameter is mixed with a suspension of magnetic capped Janus motors. Manipulation of the cargo (uploading, transportation, and delivery) is realized by applying an external magnetic field that plays in this case a dual role: (i) it reorients the magnetic caps, enabling the directed motion of Janus particles, and (ii) induces a net magnetic moment for the superparamagnetic cargo beads. The targeted delivery is possible due to manipulation of the magnetic dipole−dipole interactions between the magnetic moments of the cargo and the Janus particles. This interaction can be switched from attractive to repulsive and back by changing the orientation of the external magnetic field. In particular, when the magnetic field is applied in the plane, the interaction between magnetic moments m_1 and m_2 of the Janus particle and the superparamagnetic cargo, respectively, is attractive. This ensures a simple procedure to upload and transport the cargo using Janus motors. By applying an out-of-plane magnetic field (along *z*-axis), the dipolar magnetic moments m_1 and m_2 align perpendicularly to the substrate. The resulting repulsive interaction leads to a release (delivery) of the cargo from the magnetic particle.

The transport of the superparamagnetic chemically inert cargo by means of catalytic magnetic Janus particles is analyzed by comparing the time evolution of the velocities of both particles (Figure 3). The experiment is performed in a 10 wt % hydrogen peroxide solution in an applied magnetic field with a magnitude of 40 Oe. A stronger magnetic field compared with previous experiments is required in order to ensure a sufficiently large magnetic moment of the superparamagnetic cargo for the cargo-motor composite to be firmly attached during transportation. Three regions are clearly identified with respect to the values of velocity in Figure 3: (i) approach of the Janus particle to the cargo; (ii) upload and transportation; and (iii) release of the cargo. At the first stage (region: *Approach*), the single Janus particle moves with a velocity of about 6 μm/s. This value is close to that

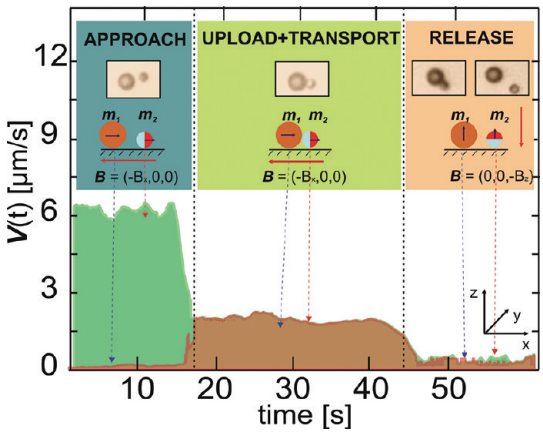

Figure 3. Targeted delivery of a superparamagnetic cargo particle: time evolution of the velocity of an individual Janus engine and a "Janus particle−cargo" pair. The velocity of the Janus particle drops after cargo is uploaded. Release of the cargo is realized by changing the magnetic field orientation from in-plane to out-of-plane.

measured for free single Janus particle (Figure 2a). The velocity of the superparamagnetic bead during the approach stage is close to zero, which is expected for a particle that is not catalytically active and undergoes thermal fluctuations. When the Janus particle is in the vicinity of the cargo, the magnetic attractive interaction leads to sticking of the two particles; that is, uploading of the cargo takes place. After uploading, the bead moves with the Janus particle as a single object. This results in a substantial decrease of the velocity of the Janus particle down to 2 μm/s (region: *Upload + Transport*), which is maintained during the whole transportation stage (Supporting Information, Movie 3). Once the cargo is transported to the desired location, it is released by turning the magnetic field normal to the substrate. At this stage, both particles stop their motion: the cargo stops, because it is chemically inactive, and the Janus particle stops, because its catalytic cap is aligned perpendicularly to the substrate (region: *Release*, and Supporting Information, Movie 4). Thus, the complete scheme of targeted delivery is demonstrated using catalytic Janus engines.

Sorting of Microscopic Objects in the Microchannel Structure. Catalytic magnetic Janus motors can be utilized for diverse applications in lab-on-a-chip technologies.[50−52] They perform advanced tasks like transportation of the molecular species to relevant places and serve for the sorting of microobjects, particles, cells, and emulsion droplets. In the following experiment, we bring the catalytic particles into a microfluidic chip and demonstrate their performance for the following applications: (i) manipulation of the free catalytic particles; (ii) transportation of the cargo particles through the channel; (iii) sorting of the particles between the channels (Figure 4). For this purpose, we produce microfluidic channels by structuring the glass slides

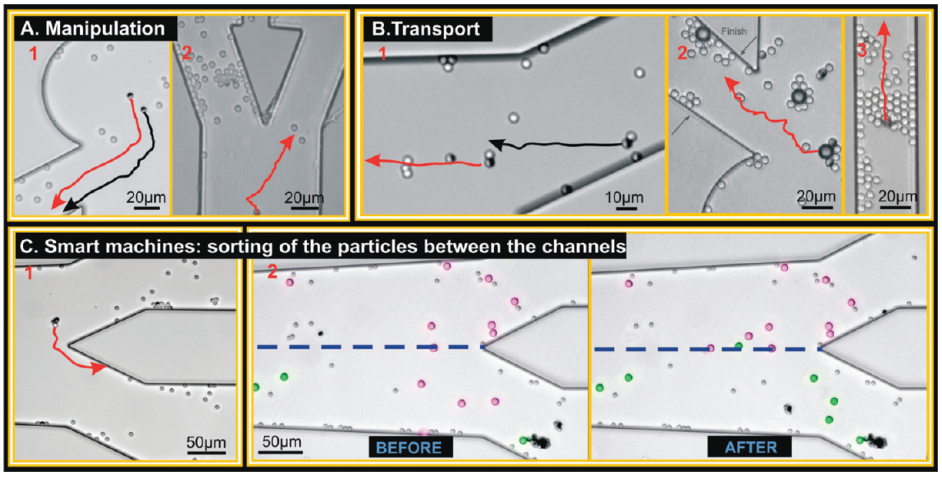

Figure 4. Janus micromotors on microfluidic chip: (a) manipulation of single magnetic Janus motors by means of application of an external magnetic field; (b) catalytic motors transport the colloidal cargo through the microfluidic channel (snap 1 transportation of single particle; snap 2 transportation of the superparamagnetic bead; snap 3 transportation of the colloidal assembly); (c) sorting concept of the particles (snap 1 plain silica and snap 2 superparamagnetic beads) between the channels is demonstrated.

with negative SU-8 resist and UV lithography. The designed structures consist of a reservoir that expands into channels, as required for particle selection (Methods). Next, a 100-nm-thick SiO_2 film is deposited onto the resist to protect the patterned channel structure from the H_2O_2 action. The width of the channels varies from 40 to 200 μm depending on the application, while the height is fixed to 20 μm. Afterward, we prepare mixtures of catalytically active magnetic Janus particles in the 10 wt % aqueous H_2O_2 solution with inert cargo particles: (i) plain silica with a diameter of 5 μm (Figure 4a,b) or (ii) fluorescent superparamagnetic beads with a diameter of 8 μm (Figure 4c, right panels). Thereafter, 20 μL of the suspension is dripped onto the patterned glass substrate and finally covered by the thin glass slide. A small external magnetic field (3 Oe) is applied to manipulate the motion of the catalytic particles. Figure 4a displays the corresponding optical microscope images of the Janus motors located in the microreservoir (snaps 1 and 2). By changing the orientation of the magnetic field, the particles were further transported toward selected channels (Supporting Information, Movies 5 and 6), as depicted by the trajectories. The controlled transport of the spherical cargo in microfluidic channels using catalytic Janus motors is demonstrated in Figure 4b. While snap 1 visualizes the pulling of attached silica particles by the catalytic spheres, snaps 2 and 3 demonstrate the ability to perform more complex tasks, that is, a transport of the superparamagnetic bead (Supporting Information, Movie 7), and pushing of the colloidal assembly through the narrow channel (Supporting Information, Movie 8).

The combination of manipulation and transport of objects using catalytic Janus particles allows the possibility to *sort* the microobjects between different channels (Figure 4c). Snap 1 demonstrates the sorting of a single particle, performed by a Janus motor from the upper channel to the lower one. This concept is applied in the following to sort the green and pink-colored fluorescent particles into different channels (snap 2). The first image (indicated "BEFORE") illustrates the initial state of randomly distributed fluorescent particles in the structure, while the second one (indicated "AFTER") shows their final distributions after the sorting procedure is completed. The sorting is realized by selective transportation of the green-colored fluorescent beads to the lower channel. The upload and release of the particles is realized according to the previously described approach (Figure 3). The experiments were performed using multichannel fluorescent module incorporated into the inverted microscope.

CONCLUSION

We fabricated catalytic Janus motors with specially designed magnetic properties of the cap structure exhibiting a well-defined magnetic easy axis that coincides with the symmetry axis of the cap. This magnetic configuration allows full control over the motion of the Janus particle and provides a direct manipulation of the cargo (upload, transport, delivery) by applying spatially varying magnetic fields. The capabilities of the magnetic Janus particles were demonstrated by employing them for manipulation, transportation, and sorting of microobjects in microfluidic channels.

This concept can be extended to perform various tasks including application-relevant cleaning of multicomponent or contaminated fluids. Using catalytic engines for transport and sorting of species is also of

interest in many life-science-related areas, for example, development of drug delivery agents[12] and biosensors.[53,54] Nevertheless, the system in its current state has a number of limitations. All approaches reported on catalytically driven artificial motors still suffer from incompatibility of the H_2O_2-based reaction with biological systems, since hydrogen peroxide is a strong oxidizing agent and harmful for most of biological tissues and living cells at these working conditions. Thus, the substantial decrease of the working concentrations of hydrogen peroxide,[55] using more efficient catalysts like enzymes[18] or switching to other fuel sources is necessary to meet the requirements of biocompatibility. Finding the optimal conditions to use the catalytic artificial engines for biological purposes still remains a challenging task for future applications.

METHODS

Self-Assembled Monolayers of SiO_2 Particles. Preparation of nonmagnetic particle monolayers was carried out following the procedure initially proposed by Micheletto *et al.*[45] In this case, a droplet of a particle/water solution is deposited onto a cleaned thermally oxidized Si(100) wafer. The cleaning involves ultrasonication in acetone, ethanol, and purified water followed by treatment in oxygen plasma for 4 min. Afterward, the droplet evaporates in a small and tilted box, leading to the self-assembling of the particle monolayers. By varying the concentration of particles in the colloid solution, the tilting angle and the size of the droplet, a sufficient coverage of the substrate with particle monolayers is possible.[56,57]

Deposition of Metal Films. $[Co/Pt(Pd)]_N$ multilayers is a convenient model system as their magnetic anisotropy can be easily varied by adjusting the individual Co layer thickness. Perpendicular magnetic anisotropy occurs in a certain range of Co thickness where the interface anisotropy is sufficiently large to overcome the shape anisotropy.[58] The deposition of the multilayer stacks and magnetic materials was done by using magnetron sputtering at a base pressure of 1×10^{-7} mbar. Co and Pt were sputtered in an Ar pressure of 8×10^{-3} mbar at a rate of 0.5 Å/s. No postannealing of the samples was applied. After deposition, the samples were magnetically saturated in the out-of-plane direction resulting in a well-defined orientation of magnetic moment along the main symmetry axis of the cap.

Fabrication of Microfluidic Channels. First, a 20-μm-thick film of the negative SU-8 2010 photoresist (MicroChem) was prepared on the glass slides by spin-coating with a constant speed of 4000 rpm. Microfluidic channels were further produced by patterning the photoresist film using UV lithography. To protect the organic photoresist from the destructive action of the hydrogen peroxide, a 100-nm-thick SiO_2 film was deposited onto the polymeric film. The oxide was deposited by means of electron beam vapor deposition at a base pressure of 1×10^{-6} mbar.

Reagents. Aqueous solution of hydrogen peroxide was prepared by subsequent dilution (volume/volume) of the stock solution of hydrogen peroxide (30 wt %, Sigma Aldrich) with deionized water.

Characterization of the Motion of Catalytic Particles. The mean velocity V_{mean} in Figure 2a is determined as follows: (a) trajectories of the moving particles are recorded; (b) the instantaneous velocity along the trajectory is obtained as the time derivative of the arc length, and shows a fluctuating behavior around a value $\langle V(t) \rangle$; (c) the mean velocity V_{mean} (Figure 2a) is derived by averaging the velocities $\langle V(t) \rangle$ corresponding to the various recorded trajectories (six for each concentration). The error bars indicate the deviation from this average.

Conflict of Interest: The authors declare no competing financial interest.

Acknowledgment. The authors thank C. Krien for layer deposition; Dr. S. Baunack for electron microscopy images; S. Harazim for helping in the setting up of microfluidic experiments. The work was financially supported in part *via* the grant from Volkswagen Foundation [Grant No. (I/8072)] and German Science Foundation (DFG, Grant No. MA 5144/1-1).

Supporting Information Available: Quality of the array of capped Janus particles and statistical analysis of their mean velocities V_{mean}; Movies 1−10 that demonstrate various aspects of motion of catalytic Janus motors and their applications for targeted delivery of various objects. This material is available free of charge *via* the Internet at http://pubs.acs.org.

REFERENCES AND NOTES

1. Soong, R. K.; Bachand, G. D.; Neves, H. P.; Olkhovets, A. G.; Craighead, H. G.; Montemagno, C. D. Powering an Inorganic Nanodevice with a Biomolecular Motor. *Science* **2000**, *290*, 1555–1558.
2. Leigh, D. A.; Zerbetto, F.; Kay, E. R. Synthetic Molecular Motors and Mechanical Machines. *Angew. Chem., Int. Ed.* **2007**, *46*, 72–191.
3. Leong, T. G.; Randall, C. L.; Benson, B. R.; Bassik, N.; Stern, G. M.; Gracias, D. H. Tetherless Thermobiochemically Actuated Microgrippers. *Proc. Natl. Acad. Sci. U.S.A.* **2009**, *106*, 703–708.
4. Dreyfus, R.; Baudry, J.; Roper, M. L.; Fermigier, M.; Stone, H. A.; Bibette, J. Microscopic Artificial Swimmers. *Nature* **2005**, *437*, 862–865.
5. Ozin, G. A.; Manners, I.; Fournier-Bidoz, S.; Arsenault, A. Dream Nanomachines. *Adv. Mater.* **2005**, *17*, 3011–3018.
6. Mallouk, T. E.; Sen, A. Powering Nanorobots. *Sci. Am.* **2009**, *300*, 72–77.
7. Ghosh, A.; Fischer, P. Controlled Propulsion of Artificial Magnetic Nanostructured Propellers. *Nano Lett.* **2009**, *9*, 2243–2245.
8. Tierno, P.; Reddy, S. V.; Yuan, J.; Johansen, T. H.; Fischer, T. M. Transport of Loaded and Unloaded Microcarriers in a Colloidal Magnetic Shift Register. *J. Phys. Chem. B* **2007**, *111*, 13479–13482.
9. Sanchez, S.; Solovev, A. A.; Schulze, S.; Schmidt, O. G. Controlled Manipulation of Multiple Cells Using Catalytic Microbots. *Chem. Commun.* **2011**, *47*, 698–700.
10. Kagan, D.; Campuzano, S.; Balasubramanian, S.; Kuralay, F.; Flechsig, G.-U.; Wang, J. Functionalized Micromachines for Selective and Rapid Isolation of Nucleic Acid Targets from Complex Samples. *Nano Lett.* **2011**, *11*, 2083–1087.
11. Kreuter, J. *Colloidal Drug Delivery Systems*; Dekker: New York, 1994.
12. Irwin, D. J. Drug Delivery: One Nanoparticle, One Kill. *Nat. Mater.* **2011**, *10*, 342–343.
13. Paxton, W. F.; Kistler, K. C.; Olmeda, C. C.; Sen, A., St.; Angelo, S. K.; Cao, Y.; Mallouk, T. E.; Lammert, P. E.; Crespi, V. H. Catalytic Nanomotors: Autonomous Movement of Striped Nanorods. *J. Am. Chem. Soc.* **2004**, *126*, 13424–13431.
14. Paxton, W. F.; Sundararajan, S.; Mallouk, T. E.; Sen, A. Chemical Locomotion. *Angew. Chem., Int. Ed.* **2006**, *45*, 5420–5429.
15. Dhar, P.; Fischer, T. M.; Wang, Y.; Mallouk, T. E.; Paxton, W. F.; Sen, A. Autonomously Moving Nanorods at a Viscous Interface. *Nano Lett.* **2006**, *6*, 66–72.
16. Ismagilov, R. F.; Schwartz, A.; Bowden, N.; Whitesides, G. M. Autonomous Movement and Self-Assembly. *Angew. Chem., Int. Ed.* **2002**, *41*, 652–654.
17. Solovev, A. A.; Mei, Y. F.; Bermúdez Ureña, E.; Huang, G. S.; Schmidt, O. G. Catalytic Microtubular Jet Engines

Self-Propelled by Accumulated Gas Bubbles. *Small* **2009**, *5*, 1688–1692.
18. Sanchez, S.; Solovev, A. A.; Mei, Y. F.; Schmidt, O. G. Dynamics of Biocatalytic Microengines Mediated by Variable Friction Control. *J. Am. Chem. Soc.* **2010**, *132*, 13144–13145.
19. Pumera, M. Electrochemically Powered Self-Propelled Electrophoretic Nanosubmarines. *Nanoscale* **2010**, *2*, 1643–1649.
20. Balasubramanian, S.; Kagan, D.; Hu, C. J.; Campuzano, S.; Lobo-Castañon, M.; Lim, N.; Kang, D. Y.; Zimmerman, M.; Zhang, L.; Wang, J. Micromachine-Enabled Capture and Isolation of Cancer Cells in Complex Media. *Angew. Chem., Int. Ed.* **2011**, *50*, 4161–4164.
21. Howse, J. R.; Jones, R. A. L.; Ryan, A. J.; Gough, T.; Vafabakhsh, R.; Golestanian, R. Self-Motile Colloidal Particles: From Directed Propulsion to Random Walk. *Phys. Rev. Lett.* **2007**, *99*, 048102 (4 pages).
22. Wheat, P. M.; Marine, N. A.; Moran, J. L.; Posner, J. D. Rapid Fabrication of Bimetallic Spherical Motors. *Langmuir* **2010**, *26*, 13052–13055.
23. Okano, K.; Takahashi, S.; Yasuda, K.; Tokinaga, D.; Imai, I.; Koga, M. Using Microparticle Labeling and Counting For Attomole-Level Detection in Heterogeneous Immunoassay. *Anal. Biochem.* **1992**, *202*, 120–125.
24. Salata, O. V. Applications of Nanoparticles in Biology and Medicine. *J. Nanobiotechnol.* **2004**, *2*, 3 (6 pages).
25. Baudry, J.; Rouzeau, C.; Goubault, C.; Robic, C.; Cohen-Tannoudji, L.; Koenig, A.; Bertrand, E.; Bibette, J. Acceleration of the Recognition Rate Between Grafted Ligands and Receptors with Magnetic Force. *Proc. Natl. Acad. Sci. U.S.A.* **2006**, *103*, 16076–16078.
26. Barbé, C.; Bartlett, J.; Kong, L.; Finnie, K.; Lin, H. Q.; Larkin, M.; Calleja, S.; Bush, A.; Calleja, G. Silica Particles: A Novel Drug-Delivery System. *Adv. Mater.* **2004**, *16*, 1–8.
27. Valadares, L. F.; Tao, Y. G.; Zacharia, N. S.; Kitaev, V.; Galembeck, F.; Kapral, R.; Ozin, G. A. Catalytic Nanomotors: Self-Propelled Sphere Dimers. *Small* **2010**, *6*, 565–572.
28. Baraban, L.; Tasinkevych, M.; Popescu, M. N.; Sanchez, S.; Dietrich, S.; Schmidt, O. G. Transport of Cargo by Catalytic Janus Micro-motors. *Soft Matter* **2012**, *8*, 48–52.
29. Solovev, A. A.; Sanchez, S.; Pumera, M.; Mei, Y. F.; Schmidt, O. G. Magnetic Control of Tubular Catalytic Microbots for the Transport, Assembly, and Delivery of Micro-objects. *Adv. Func. Mater.* **2010**, *20*, 2430–2435.
30. Kline, T. R.; Paxton, W. F.; Mallouk, T. E.; Sen, A. Catalytic Nanomotors: Remote-Controlled Autonomous Movement of Striped Metallic Nanorods. *Angew. Chem., Int. Ed.* **2005**, *44*, 744–746.
31. Terris, B. D. Fabrication Challenges for Patterned Recording Media. *J. Magn. Magn. Mater.* **2009**, *321*, 512–517.
32. Piramayagam, S. N.; Srinivasan, K. Recording Media Research for Future Hard Disk Drives. *J. Magn. Magn. Mater.* **2009**, *321*, 485–494.
33. Wood, R. Future Hard Disk Drive Systems. *J. Magn. Magn. Mater.* **2009**, *321*, 555–561.
34. Makarov, D.; Baraban, L.; Guhr, I. L.; Boneberg, J.; Schift, H.; Gobrecht, J.; Schatz, G.; Leiderer, P.; Albrecht, M. Arrays of Magnetic Nanoindentations with Perpendicular Anisotropy. *Appl. Phys. Lett.* **2007**, *90*, 093117 (3 pages).
35. Bermúdez-Ureña, E.; Mei, Y. F.; Coric, E.; Makarov, D.; Albrecht, M.; Schmidt, O. G. Deterministic Fabrication of Ferromagnetic Rolled-Up Microtubes and Their Nonlinear Rotational Dynamics. *J. Phys. D: Appl. Phys* **2009**, *42*, 055001 (9 pages).
36. Makarov, D.; Lee, J.; Brombacher, C.; Schubert, C.; Fuger, M.; Suess, D.; Fidler, J.; Albrecht, M. Perpendicular FePt-Based Exchange-Coupled Composite Media. *Appl. Phys. Lett.* **2010**, *96*, 062501 (3 pages).
37. Smith, E. J.; Makarov, D.; Sanchez, S.; Fomin, V. M.; Schmidt, O. G. Magnetic Micro-helix Coil Structures. *Phys. Rev. Lett.* **2011**, *107*, 097204 (4 pages).
38. Albrecht, M.; Hu, G.; Guhr, I. L.; Ulbrich, T. C.; Boneberg, J.; Leiderer, P.; Schatz, G. Magnetic Multilayers on Nanospheres. *Nat. Mater.* **2005**, *4*, 203–206.
39. Ulbrich, T. C.; Makarov, D.; Hu, G.; Guhr, I. L.; Suess, D.; Schrefl, T.; Albrecht, M. Magnetization Reversal in a Novel Gradient Nanomaterial. *Phys. Rev. Lett.* **2006**, *96*, 077202 (4 pages).
40. Baraban, L.; Makarov, D.; Albrecht, M.; Rivier, N.; Leiderer, P.; Erbe, A. Frustration-Induced Magic Number Clusters of Colloidal Magnetic Particles. *Phys. Rev. E* **2008**, *77*, 031407 (6 pages).
41. Ulbrich, T. C.; Bran, C.; Makarov, D.; Hellwig, O.; Risner-Jamtgaard, J. D.; Yaney, D.; Rohrmann, H.; Neu, V.; Albrecht, M. The Effect of Magnetic Coupling on the Magnetization Reversal in Arrays of Magnetic Nanocaps. *Phys. Rev. B* **2010**, *81*, 054421 (7 pages).
42. Günther, C. M.; Hellwig, O.; Menzel, A.; Pfau, B.; Radu, F.; Goncharov, A.; Makarov, D.; Albrecht, M.; Schlotter, W. F.; Rick, R.; *et al.* Microscopic Reversal Behavior of Magnetically Capped Nanospheres. *Phys. Rev. B* **2010**, *81*, 064411 (7 pages).
43. Sundararajan, S.; Lammert, P. E.; Zudans, A. W.; Crespi, V. H.; Sen, A. Catalytic Motors for Transport of Colloidal Cargo. *Nano Lett.* **2008**, *8*, 1271–1276.
44. Burdick, J.; Laocharoensuk, R.; Wheat, P. M.; Posner, J. D.; Wang, J. Synthetic Nanomotors in Microchannel Networks: Directional Microchip Motion and Controlled Manipulation of Cargo. *J. Am. Chem. Soc.* **2008**, *130*, 8164–8165.
45. Micheletto, R.; Fukuda, H.; Ohtsu, M. A Simple Method for the Production of a Two-Dimensional, Ordered Array of Small Latex Particles. *Langmuir* **1995**, *11*, 3333–3336.
46. Mei, Y. F.; Solovev, A. A.; Sanchez, S.; Schmidt, O. G. Rolled-Up Nanotech on Polymers: From Basic Perception to Self-Propelled Catalytic Microengines. *Chem. Soc. Rev.* **2011**, *40*, 2109–2119.
47. Köppl, M.; Henseler, P.; Erbe, A.; Nielaba, P.; Leiderer, P. Layer Reduction in Driven 2D-Colloidal Systems through Microchannels. *Phys. Rev. Lett.* **2006**, *97*, 208302 (4 pages).
48. Popescu, M. N.; Dietrich, S.; Tasinkevych, M.; Ralston, J. Phoretic Motion of Spheroidal Particles Due to Self-Generated Solute Gradients. *Eur. Phys. J. E* **2010**, *31*, 351–367.
49. Ebbens, S. J.; Howse, J. R. In Pursuit of Propulsion at the Nanoscale. *Soft Matter* **2010**, *6*, 726–738.
50. De Mello, A. J. Control and Detection of Chemical Reactions in Microfluidic Systems. *Nature* **2006**, *442*, 394–402.
51. Sanchez, S.; Solovev, A. A.; Harazim, S. M.; Schmidt, O. G. Microbots Swimming in the Flowing Streams of Microfluidic Channels. *J. Am. Chem. Soc.* **2011**, *133*, 701–703.
52. Baraban, L.; Bertholle, F.; Salverda, M.; Bremond, N.; Panizza, P.; Baudry, J.; de Visser, J. A.; Bibette, J. Millifluidic droplet analyser for microbiology. *Lab Chip* **2011**, *11*, 4057–4062 (5 pages).
53. Melzer, M.; Karnaushenko, D.; Makarov, D.; Baraban, L.; Calvimontes, A.; Mönch, I.; Kaltofen, I.; Mei, Y; Schmidt, O. G. Elastic magnetic sensor with isotropic sensitivity for inflow detection of magnetic objects. *RSC Adv.* **2012**, *2*, 2284–2288 (4 pages).
54. Moench, I.; Makarov, D.; Koseva., R.; Baraban, L.; Karnaushenko, D.; Kaiser, K.; Arndt, K. F.; Schmidt, O. G. Rolled-up Magnetic Sensor: Nanomembrane Architecture for In-Flow Detection of Magnetic Objects. *ACS Nano* **2011**, *5*, 7436–7442.
55. Sanchez, S.; Ananth, A. N.; Fomin, V.; Viehrig, M.; Schmidt, O. G. Superfast Motion of Catalytic Microjet Engines at Physiological Temperature. *J. Am. Chem. Soc.* **2011**, *133*, 14860–14863.
56. Brombacher, C.; Saitner, M.; Pfahler, C.; Plettl, A.; Ziemann, P.; Makarov, D.; Assmann, D.; Siekman, M.; Abelmann, L.; Albrecht, M. Tailoring Particle Arrays by Isotropic Plasma Etching: An Approach Towards Percolated Perpendicular Media. *Nanotechnology* **2009**, *20*, 105304 (5 pages).
57. Makarov, D.; Bermúdez-Ureña, E.; Schmidt, O. G.; Liscio, F.; Maret, M.; Brombacher, C.; Schulze, S.; Hietschold, M.; Albrecht, M. Nanopatterned CoPt Alloys with Perpendicular Magnetic Anisotropy. *Appl. Phys. Lett.* **2008**, *93*, 153112 (3 pages).
58. Carcia, P. F.; Meinhaldt, A. D.; Suna, A. Perpendicular Magnetic Anisotropy in Pd/Co Thin Film Layered Structures. *Appl. Phys. Lett.* **1985**, *47*, 178 (3 pages).